Prediction of Bond Wire Fatigue of IGBTs in a PV Inverter Under a Long-Term Operation

Paula Diaz Reigosa, *Student Member, IEEE*, Huai Wang, *Member, IEEE*, Yongheng Yang, *Member, IEEE*, and Frede Blaabjerg, *Fellow, IEEE*

***Abstract*—Bond wire fatigue is one of the dominant failure mechanisms in insulated-gate bipolar transistor (IGBT) modules under cyclic stresses. However, there are still major challenges ahead to achieve a realistic bond wire lifetime prediction in field operation. This paper proposes a Monte Carlo based analysis method to predict the lifetime consumption of bond wires of IGBT modules in a photovoltaic (PV) inverter. The variations in IGBT parameters (e.g., on-state collector–emitter voltage), lifetime models, and environmental and operational stresses are taken into account in the lifetime prediction. The distribution of the annual lifetime consumption is estimated based on a long-term annual stress profile of solar irradiance and ambient temperature. The proposed method enables a more realistic lifetime prediction with a specified confidence level compared to the state-of-the-art approaches. A study case of IGBT modules in a 10-kW three-phase PV inverter is given to demonstrate the procedure of the method. The obtained results of the lifetime distribution can be used to justify the selection of IGBTs for the PV inverter applications and the corresponding risk of unreliability.**

***Index Terms*—Bond wire fatigue, insulated-gate bipolar transistor, mission profile, Monte Carlo methods, reliability.**

I. Introduction

A substantial effort is in place to the reliability and the associated maintenance cost of grid-connected transformerless photovoltaic (PV) inverters in recent years [1], [2]. It is a challenge to fulfill the product design specifications with ever-increasing lifetime requirements and more stringent cost constraints [3], [4]. Many efforts have been devoted to the reliability study of PV power conversion systems [5]–[11]. One aspect of study is on the reliability issues from the control perspective, especially the islanding control and the maximum power point tracking [12]. The other aspect is on the system-level reliability prediction. Many of the reliability prediction methods are based on the component-level reliability information provided in the Military-Handbook-217F [13], such as those presented in [5]–[7] and [9]. The reliability data in this handbook are simple to be used but could be inappropriate for electronic components, since they are based on an assumption of constant failure rates (i.e., wear out is not included) as discussed in detail in [14]. In [6] and [8], the component-level reliability information is based on the guide FIDES [15], which provides the acceleration factors of different stressors (e.g., temperature and humidity) and includes also the wear out failure mechanisms of electronic components. The data in FIDES are still relatively general to a certain type of components (e.g., insulated-gate bipolar transistors (IGBTs), capacitors, and resistors), without the differentiation of technologies and manufacturers. To have an improved reliability prediction, the impact of the loading conditions has been considered in [6], [8], [10], and [11]. However, it is quite challenging to have a realistic system-level reliability prediction due to the lack of more specific component-level reliability analyses.

A reliability analysis of the PV systems components is indispensable in order to identify the weakest components; according to a survey based on field experiences from power electronics manufacturers, about 31% of the 56 responders consider power semiconductor devices as the most fragile components [16]. IGBTs are the commonly used semiconductor devices in PV inverters; however, the reliability analysis of the IGBTs designed in PV inverters is usually not well treated. One of the dominant failure mechanisms of IGBT modules is the bond wire fatigue due to temperature excursions [17], [18]. The ambient temperature variation and the self-heating of IGBTs contribute to these temperature excursions.

The lifetime prediction methods of IGBT bond wires can be classified into three categories. The first category is based on constant failure rate models from various handbooks, for example, the Military-Handbook-217F [13], [14]. This method is simple but inappropriate, since it is based on an assumption of constant failure rates and the impact of temperature excursions is not considered. Even though it is still used in the literature, the Military-Handbook-217F has been cancelled in 1995. An updated version, the Military-Handbook-217H, is under discussion [19] based on a more physics-based method. The second category is based on empirical lifetime models developed mainly from accelerated lifetime testing data [20]–[23]. It is the most widely used method for the lifetime prediction of IGBT modules. The main drawback of empirical lifetime models is that they are obtained from statistical analysis of available lifetime data, which do not directly describe the physical failure mechanisms. The use of these lifetime models should be justified in terms of applicability, limitations, and the underlying statistical properties. The third category is based on physics-of-failure (PoF) lifetime models, which are obtained by modeling the stress–strain deformations due to thermal–mechanical stresses [24]. The PoF method provides a better insight in the physical mechanisms that cause the bond wire fatigue in IGBT modules. However, the use of PoF-based lifetime models is still limited due to the lack of detailed information of the materials and

Manuscript received January 26, 2015; revised May 12, 2015 and August 25, 2015; accepted December 7, 2015. Date of publication December 17, 2015; date of current version May 20, 2016. Recommended for publication by Associate Editor F. H. Khan.

The authors are with the Department of Energy Technology, Aalborg University, Aalborg 9220, Denmark (e-mail: pdr@et.aau.dk; hwa@et.aau.dk; yoy@et.aau.dk; fbl@et.aau.dk).

Color versions of one or more of the figures in this paper are available online at http://ieeexplore.ieee.org.

Digital Object Identifier 10.1109/TPEL.2015.2509643

geometries of IGBT modules. It is still an open question on how to introduce statistics into the PoF-based lifetime models of IGBT modules to incorporate the variations and uncertainties, besides the deterministic physical properties. In this paper, a well-justified empirical lifetime model of IGBT bond wires will be used for the proposed method.

The challenges to predict the IGBT lifetime in PV inverters lie in the following aspects: 1) it is necessary to differentiate various fatigue failure mechanisms and failure sites (e.g., bond wires and solder joints) [25], [26]; 2) each lifetime model has its limitations due to specific technologies, failure mechanisms, and certain environmental and operational stresses (e.g., temperature range, cycle time of temperature excursions) [23]; 3) the stress levels of IGBTs vary with the mission profiles (i.e., solar irradiance and ambient temperature during the life cycle) due to the intermittent solar power [27], [28]; and 4) the end-of-life of a population of IGBTs with the same product part number varies in field operations due to variances in manufacturing process and statistical properties of the lifetime models.

The research in [24], [29], and [30] discusses the differentiation of various failure mechanisms and reveals that the power cycling with heating time (i.e., the period where power losses are generated in the device resulting in a temperature rise) below 1 min has a significant effect on the fatigue of bond wires. Moreover, a long-term mission profile, which has been presented in [31] and [32], has been adopted. However, there is still a lack of study on the effect of variances in IGBT parameters (e.g., on-state collector–emitter voltage) and statistical properties of lifetime models. The relevant variances in IGBT lifetime prediction in PV applications can be classified into: 1) variances in environmental and operational stresses (e.g., the solar irradiance and ambient temperature); 2) variances in empirical lifetime models introduced by the statistical life data analysis to derive the lifetime models; 3) variances in IGBT electrical parameters and thermal parameters due to the variations in manufacturing processes; and 4) variances in time-dependent parameters due to IGBT degradation.

The Monte Carlo method can be applied to take into account the above variances. It has been applied for other reliability aspects, as discussed in [33]–[36]. In [33], the statistical properties of temperature and humidity are considered in a deterministic PoF lifetime model by Monte Carlo simulations. In [34] and [35], the impact of the geometry parameters of an IGBT power module is simulated by applying the Monte Carlo method. An optimal design of the parameters can, therefore, be achieved. In [36], the uncertainties of the IGBT on-state saturation voltage degradation curve are analyzed for online prognostic purpose.

In PV applications, IGBTs that can fulfill a specific lifetime requirement are usually readily available. The practical issue for PV inverter designers is how to select the IGBTs with a minimum cost and measurable risk of unreliability. This paper proposes a Monte Carlo based analysis method to study the impact of the above variances on the bond wire fatigue of IGBTs in a PV inverter. The presented study tackles the issue by predicting the bond wire lifetime distribution with a specified confidence level, allowing the accumulated failure analysis due to bond wire fatigue along with the long operation.

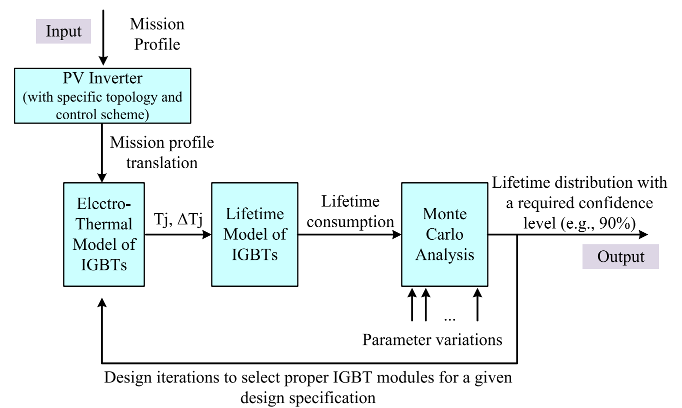

Fig. 1. Proposed Monte Carlo based method for lifetime prediction of IGBT bond wires.

This paper is organized as follows: Section II presents the proposed procedure to perform the lifetime prediction of bond wires under a long-term operation. Section III demonstrates the procedure in detail by a case study with experimental tests on a 10-kW three-phase PV inverter, considering the variances in IGBT parameters and stresses. Finally, concluding remarks are given.

II. Proposed Monte Carlo Based Lifetime Prediction Method

The proposed Monte Carlo based method for bond wire lifetime analysis is shown in Fig. 1. The procedure includes four major steps. A mission profile (i.e., the solar irradiance and ambient temperature) is applied as the input. The output is the lifetime of bond wires of IGBTs in PV inverters with a confidence level (e.g., 90%). The feedback loop from the output to the electrothermal model of IGBTs shows the design iterations to select the proper IGBT modules from multiple candidates. The purpose of the method is to provide a guideline to select the IGBT modules in the design phase to fulfill the reliability requirements, which is based on lifetime models and specific mission profiles. Based on the predicted results, an additional design margin will be added to select the most suitable IGBT for a given application. The detailed discussions on the procedure are provided in the following, and the flowchart in Fig. 2 gives the steps of the proposed algorithm.

A. Mission Profile Translation

In PV applications, the power semiconductor devices are exposed to varying electrical and thermal stresses due to the fluctuations of ambient temperature and solar irradiance. A representative long-term mission profile (e.g., an annual stress profile) is needed for the analysis.

According to the long-term mission profile, the power losses of power semiconductor devices are calculated by three steps.

1) *Output power of PV arrays (P_{PV}):* The output power of a given PV array configuration can be calculated according to the PV string model discussed in [27]. Its mapping relationship with the solar irradiance (SI) and ambient temperature can be obtained. For the sake of simplicity,

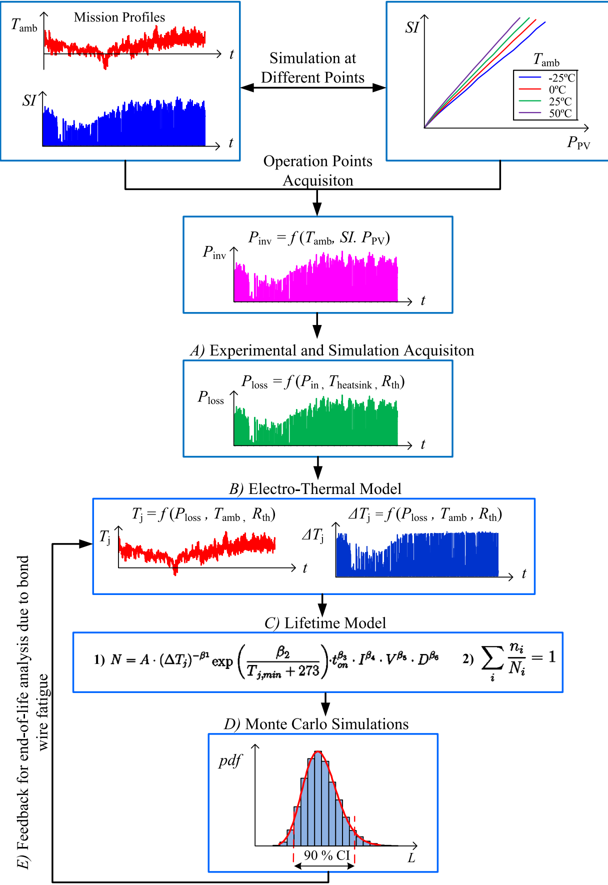

Fig. 2. Algorithm of the Monte Carlo based method for bond wire lifetime analysis: $T_{\rm amb}$—ambient temperature, $T_{\rm heatsink}$—heatsink temperature, SI—solar irradiance, $P_{\rm PV}$—output power of PV arrays, $P_{\rm inv}$—inverter input power, $P_{\rm loss}$—total inverter power loss, T_j—junction temperature, ΔT_j—junction temperature fluctuation, $R_{\rm th}$—thermal resistance, L—lifetime, pdf—probability density function, and CI—confidence interval.

four typical ambient temperature levels are used to analyze the output power profile of the PV arrays, as shown in Fig. 2. Ambient temperatures different from the four levels are approximated to the closest one.

2) *Input voltage and current of the PV inverter ($P_{\rm inv}$):* The input voltage and input current profile of the PV inverter can be derived based on the output power and the PV array configuration.
3) *Power loss profile of IGBT modules ($P_{\rm loss}$):* A mapping relationship between the power loss of the IGBT modules and the input voltage and current of the PV inverter is derived by either simulations or experimental characterizations. Then, a long-term power loss profile can be obtained by using the derived mapping relationship.

Further details of the above three steps will be discussed in Section III.

B. Electrothermal Model

An electrothermal model is applied to obtain the thermal stress of a single IGBT as shown in Fig. 3. The IGBT junction temperature T_j and its fluctuation ΔT_j can be estimated according to the method in [31], [32], and [37], where the thermal

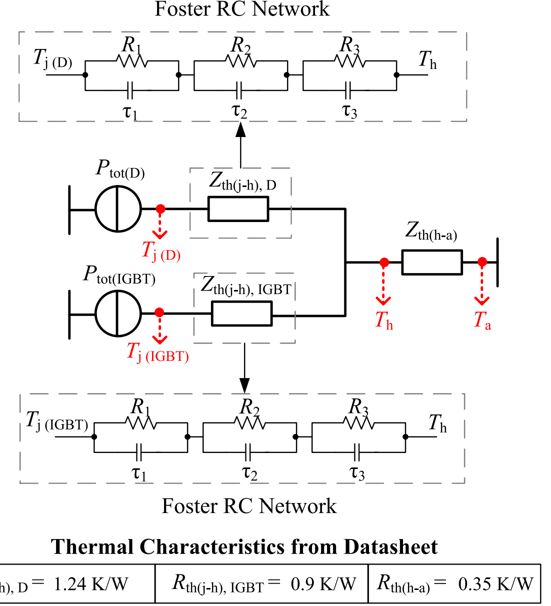

Fig. 3. Thermal model of power devices: $T_{j,({\rm IGBT})}$—IGBT junction temperature, $T_{j,(D)}$—diode junction temperature, T_h—heatsink temperature, T_a—ambient temperature, $Z_{{\rm th}(j-h),{\rm IGBT}}$—IGBT thermal impedance from junction to heatsink, $Z_{{\rm th}(j-h),D}$—diode thermal impedance from junction to heatsink, $Z_{{\rm th}(h-a)}$—thermal impedance from heatsink to ambient.

impedance from junction to heatsink, $Z_{{\rm th}(j-h)}$, is modeled as a multilayer Foster RC network. The parameters in the thermal model can be obtained by one of the following ways: 1) based on the datasheet from the IGBT module manufacturer [38]; 2) based on a simplified model from finite-element method simulation of the IGBT module [39]; and 3) based on thermal characterization of the IGBT module. The thermal impedance may increase with operation time due to the degradation of IGBT modules, which can be taken into account in the thermal analysis, as discussed in [31].

C. Lifetime Model of IGBTs

Among the three well-known dominant failure mechanisms of IGBT modules, this study focuses on the bond wire lift-off [4]. The number of cycles to failure, N_f, can be predicted based on a specific lifetime model. The best lifetime model would be from the one which considers the same testing conditions as the ones in the field operation. However, it is almost not feasible and not desirable in practice due to the time required. That is why different accelerated testing concepts have been proposed in reliability engineering for the last few decades, in order to reduce the testing time. The key point is that the selection of the lifetime model should be well justified, as discussed in more detail in Section III. For illustration purpose, an empirical lifetime model for the bond wire fatigue of IGBT modules is given below [23]

$$N_f = A \cdot (\Delta T_j)^{-\beta_1} \cdot \exp\left(\frac{\beta_2}{T_{j,\min} + 273}\right) \cdot t_{\rm on}^{\beta_3} \cdot I^{\beta_4} \cdot V^{\beta_5} \cdot D^{\beta_6} \tag{1}$$

where ΔT_j is the junction temperature fluctuation, $T_{j,\min}$ is the minimum junction temperature, $t_{\rm on}$ is the heating time of the power cycling, V is the blocking voltage of the chip, D is

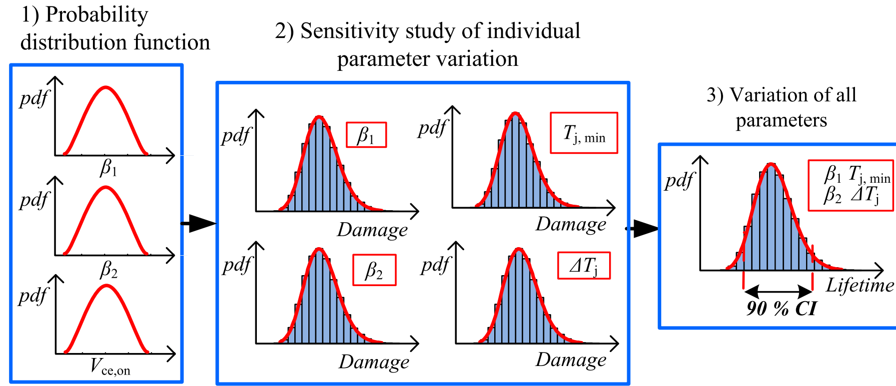

Fig. 4. Step-by-step proposed Monte Carlo analysis: β_1 and β_2—fitting coefficients of the applied lifetime model, $T_{j,\min}$—minimum junction temperature, ΔT_j—junction temperature fluctuation, $V_{\mathrm{ce,on}}$—collector–emitter voltage, pdf—probability distribution function.

the bond wire diameter, I is the current per wire, and A, β_1, β_2, β_3, β_4, β_5, and β_6 are the constant parameters as discussed in [23]. The results would be more trustable if the lifetime model parameter values are based on the true sample and working conditions; nonetheless, to reduce the testing time while obtaining meaningful lifetime models, the parameter values in [23] are widely accepted in reliability engineering.

D. Monte Carlo Analysis

The application of the lifetime model in (1) results in a fixed accumulated damage due to bond wire fatigue. It is far from reality since the IGBT parameter variations and the statistical properties of the lifetime model are not considered. In field operations, the time to end-of-life of bond wires could vary within a range due to the tolerance in physical parameters and difference in the experienced stresses. Therefore, a statistical approach based on Monte Carlo simulations is applied as shown in Fig. 4. Especially, the distributions of the temperature-related lifetime constants β_1 and β_2 and the IGBT tolerance-related parameter $V_{\mathrm{ce,on}}$ are plotted. Different values of $V_{\mathrm{ce,on}}$ result into different thermal stresses in terms of $T_{j,\min}$ and ΔT_j. Then, the sensitivity of the accumulated damage to β_1, β_2, $T_{j,\min}$, and ΔT_j can be evaluated individually or collectively. Finally, the distribution of the end-of-life of bond wires can be obtained, allowing a lifetime analysis with a specified confidence level. Further details are discussed in Section III.

E. Feedback for End-of-Life Analysis Due to Bond Wire Fatigue

Once the bond wire lifetime for a single type of IGBT has been predicted, it is possible to repeat the same procedure for several IGBTs. This method helps PV inverter designers to select the most cost-effective IGBTs, among the available options in the market for a given PV inverter application.

III. Lifetime Analysis of IGBT Bond Wires in a 10-kW PV Inverter

A case study of a 10-kW two-level voltage source inverter (2L-VSI) for PV application is discussed in this section to demonstrate the proposed method. Three IGBT modules of 1200 V/ 50 A fourth generation of IGBT technology and with aluminum bond wires are used in the PV inverter. Fig. 5 and Table I show the circuit topology and the specifications of the PV inverter, respectively. The PV inverter topology consists of a boost stage, a three-phase 2L-VSI, and a passive *LCL* filter. The current controller of the PV inverter consists of a proportional resonant controller with harmonic compensators [40]. The *LCL* filter is designed according to [41]. To perform a long-term mission profile analysis, the one-year data of solar irradiance and ambient temperature at Aalborg, Denmark, are used for the analysis [31]. The data are recorded by a mission profile logger

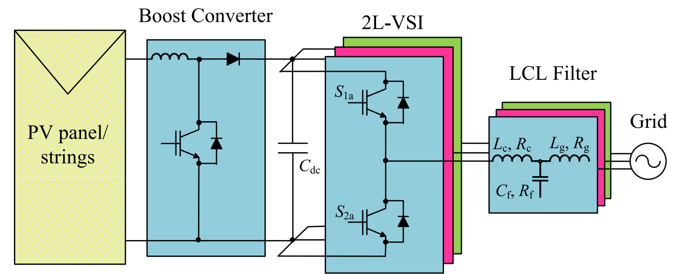

Fig. 5. 10-kW three-phase grid-connected PV system based on a 2L-VSI topology.

TABLE I
SPECIFICATIONS OF THE THREE-PHASE 2L-VSI

Three-phase 2L-VSI design ratings	
Rated Power	$P = 10$ kW
Output phase voltage	$V_n = 230$ V (RMS)
Switching frequency	$F_{\mathrm{sw}} = 7$ kHz
IGBT module power ratings	
Collector–emitter voltage	$V_{\mathrm{ce}} = 1200$ V
Collector current	$I_c = 50$ A
LCL-filter parameters	
Inverter side	$L_c = 3.6$ mH ; $R_c = 0.04\,\Omega$
Grid side	$L_g = 8.6$ mH ; $R_c = 1.72\,\Omega$
Filter capacitor	$C_f = 4.7\,\mu$F ; $R_f = 0.4\,\Omega$

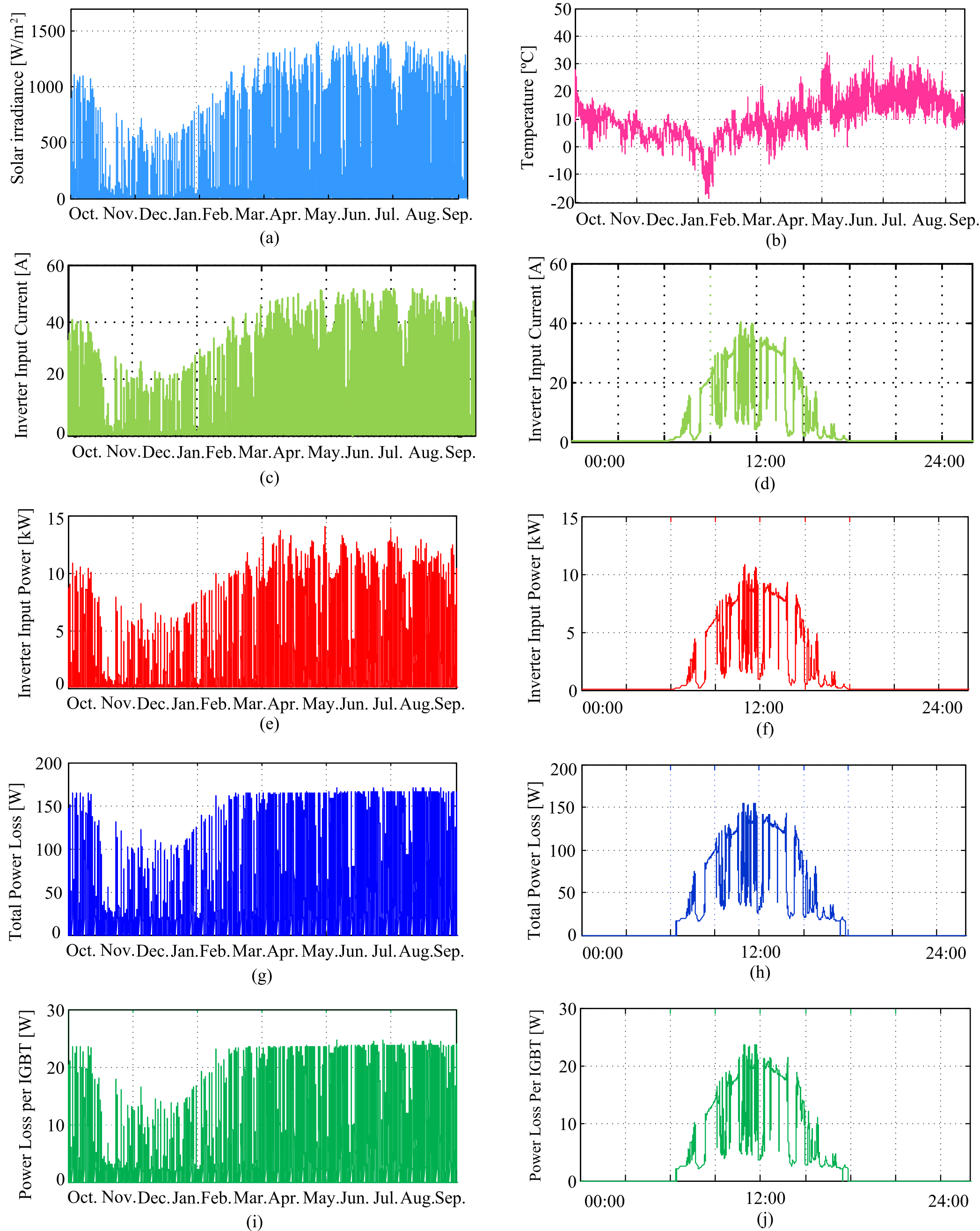

Fig. 6. Loading of a 10-kW three-phase 2L-VSI (1 s per sampling data). (a) Annual solar irradiance mission profile (SI). (b) Annual ambient temperature mission profile. (c) Annual inverter input current. (d) Daily inverter input current. (e) Annual available power from PV panels. (f) Daily available power from PV panels. (g) Annual total power loss of the IGBTs. (h) Daily total power loss of the IGBTs. (i) Annual power loss profile of single IGBT. (j) Daily power loss profile of single IGBT.

located on the roof where PV panels are located. The resolution is 1 s per data.

A. IGBT Power Loss Analysis

The IGBT power loss is analyzed by simulations under different power levels based on the electrical characteristics from the IGBT datasheet. Therefore, the relationship between the power loss and the inverter power level can be derived, enabling the translation of the annual mission profile into the power losses of the IGBT modules.

The available power from the PV panels is obtained by means of a PV string model that consists of BP365 modules, as presented in [27]. The corresponding current and voltage values for a 10-kW panel installation at four different ambient temperatures (i.e., -25 °C, 0 °C, 25 °C, and 50 °C) and 16 different solar irradiance levels (0–1500 W/m^2, with a step of 100 W/m^2) have been obtained. Fig. 6(a) and (b) shows the mission profile. Fig. 6(c) and (d) shows the annual and daily inverter current loading. Fig. 6(e) and (f) plots the annual and daily inverter input power from the PV panels based on the mission profile. To avoid the overloading of the PV inverter, the

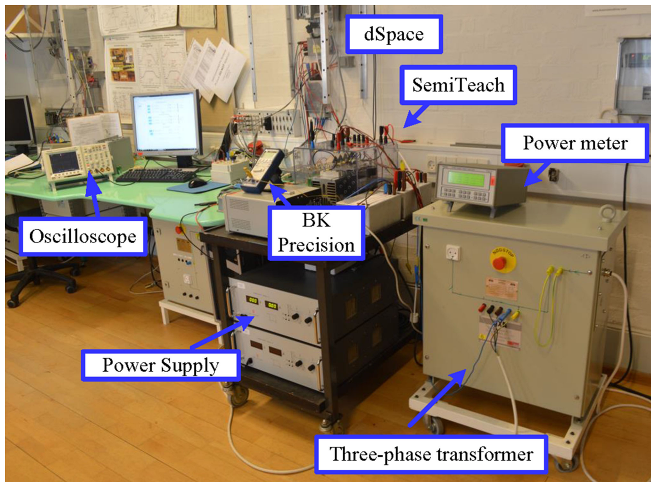

Fig. 7. Experimental setup of the three-phase 2L-VSI.

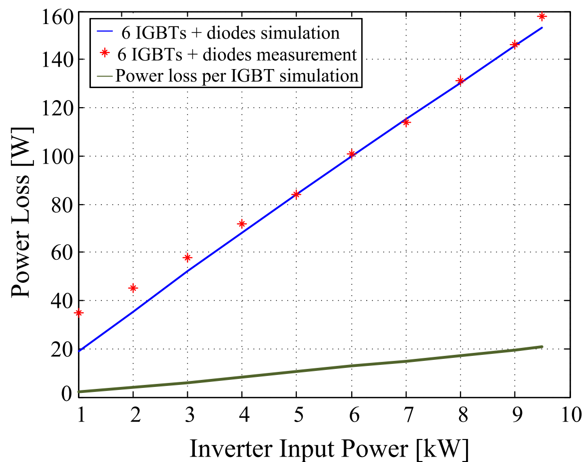

Fig. 8. Measured and simulated power losses of the inverter.

maximum power limit is set to 11 kW (i.e., 10% above the rated power).

The next step is to obtain the annual power loss of the IGBT modules. An experimental setup of the 10-kW PV inverter is built up as shown in Fig. 7. The experimental setup has been tested at different input power levels and heatsink temperatures, in order to measure the total power losses of the three IGBT modules. The total power losses of the IGBTs consisting the PV inverter can be represented as a function of the inverter input power and the heatsink temperature. The results are presented in Fig. 6(g) and (h).

Furthermore, due to the inability to measure the power losses of a single IGBT (i.e., excluding its free-wheeling diode), in the experimental setup, the 10-kW PV inverter has been analyzed by simulations in PLECS/Simulink. Since the accuracy of the translation between the mission profile and the power losses per IGBT is important, experimental results of the 10-kW PV inverter are compared with the simulation results in Fig. 8. It can be noted that the simulation results are in well agreement with the measurements, especially when the input power is above

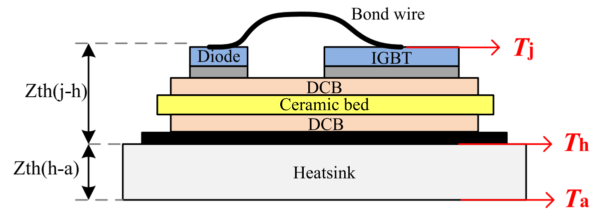

Fig. 9. Schematic cross section of an IGBT module without baseplate [24].

3 kW. Fig. 6(i) and (j) shows the annual and daily power losses of a single IGBT based on the mission profile.

B. IGBT Thermal Stress Analysis

The IGBT modules used in the PV inverter have a packaging without a base plate. Its internal structure is shown in Fig. 9 [24]. The IGBT and diode power losses flow through separate paths from the junction to the heatsink, where they merge and finally dissipate to the ambient [30].

The estimated heatsink temperature T_{heatsink} and the junction temperature T_j for one-year mission profile are shown in Fig. 10. The heatsink temperature is calculated based on the ambient temperature fluctuations from the mission profile data and the annual power losses obtained via experiments. The junction temperature is calculated based on the heatsink temperature and the power loss of a single IGBT, which has been estimated via simulations.

C. Bond Wire Lifetime Consumption Analysis

The solar irradiance and ambient temperature fluctuations cause temperature excursions of the IGBT modules. The thermal stress have two origins: the first one is power cycling which comes from load variations due to mission profiles that induce loss variations in the IGBT modules; the second one is the thermal cycling due to the variations of the ambient temperature. The IGBT power modules are, therefore, exposed to both stresses with various levels of temperature swings and frequencies. Previous studies have shown three ageing mechanisms on the bond wires: heel fractures (mechanical constraints in the wires and fatigue phenomenon due to the deformation related to temperature swings), wire bond lift-off (mechanical stress on Al–Si joints due to the difference in the thermal expansion coefficient between Al and Si), and metallurgical damage (thermomechanical stress on Al coming from the difference in the thermal expansion coefficient between Al and Si) [18], [20], [42]. According to the International Electrotechnical Commission [43], two types of cycle periods are considered: the subsecond to tens of seconds regime and the minute-range regime. Bond wire degradation strongly depends on power cycling and low-frequency thermal cycling in the subsecond to tens of seconds regime. Typically, longer cycles (e.g., above 60 s) contribute to baseplate solder degradation (if applicable) rather than bond wire degradation [44]. Consequently, the lifetime consumption in percentage of the total available life is calculated for two types of temperature stresses: power cycling due to the line frequency and thermal

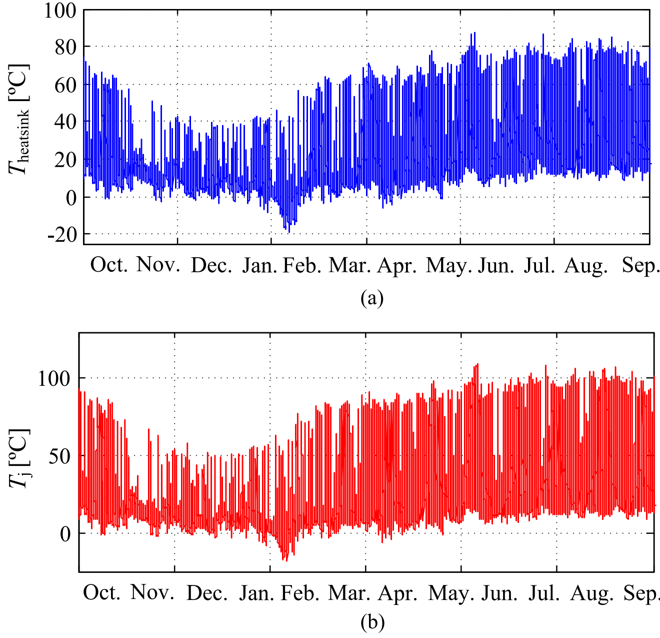

Fig. 10. Thermal loading of a single IGBT in the 2L-VSI PV inverter based on a year mission profile (1 s per sampling data). (a) Heatsink temperature. (b) IGBT junction temperature.

cycling with heating time, t_{on}, less than 60 s due to the solar irradiance (SI) and ambient temperature (T_{amb}) fluctuations. Further details are given in this section to justify the reason of the applied lifetime model and the lifetime consumption analysis.

1) Justification of the Applied Lifetime Model: An empirical model has been applied to predict the bond wire lifetime consumption for the annual mission profile. As discussed in Section I, the empirical models are easier to use because they do not require the knowledge of physical properties of the power semiconductor devices [45]. However, the use of them should be well justified.

One of the most widely used empirical lifetime models is the Coffin–Manson model shown in (2), which describes the effect of the junction temperature fluctuation ΔT_j. In this case, the lifetime is inversely proportional to the temperature swing. A and α are the curve fitting parameters [46]

$$N_f = A \times (\Delta T_j)^{-\alpha}. \quad (2)$$

The Coffin–Manson model is modified by adding the effect of the mean junction temperature T_{jm}, expressed by an Arrhenius equation [47]. E_a is the activation energy and k_b is the Boltzmann constant. The Coffin–Manson Arrhenius model is given as

$$N_f = A \times (\Delta T_j)^{-\alpha} \times \exp\left(\frac{E_a}{k_b \times T_{jm}}\right). \quad (3)$$

Nevertheless, this model does not consider the cycle heating time, which strongly affects the bond wire fatigue. The Norris–Landzberg model presented in (4) takes into account the cycle frequency f, where the exponential term β is a curve fitting parameter [48]

$$N_f = A \times f^{\beta} \times (\Delta T_j)^{-\alpha} \times \exp\left(\frac{E_a}{k_b \times T_{jm}}\right). \quad (4)$$

Finally, the Bayerer model shown in (1) includes the cycle heating time effect together with the impact of other bond wire parameters [23]. The IGBT module samples used in the acceleration testing to obtain the constants in (1) have the same technology as the ones applied in the PV inverter prototype. Moreover, comprehensive testing data are provided in [23], enabling the possibility to analyze the statistical variations of the lifetime model. Therefore, the model shown in (1) is applied in the present case study.

Since power cycling or thermal cycling with heating time t_{on} below 60 s highly contributes to the bond wire fatigue, the dependence of t_{on} as a function of the number of cycles to failure is considered according to [44], as follows:

$$\frac{N_{cyc}(t_{on})}{N_{cyc}(1.5\text{s})} = \left(\frac{t_{on}}{1.5\text{s}}\right)^{-0.3}, \qquad 0.1\,\text{s} < t_{on} < 60\,\text{s}. \quad (5)$$

2) Accumulated Damage Analysis of Line Frequency Power Cycling: There are various kinds of cumulative damage models in the literature for the reliability engineering assessment, as discussed in [49]. For the lifetime prediction of IGBT modules, the most widely used one is the Miner's rule, which is a linear cumulative damage model [50], [51]. The assumption of Miner's rule is that the damage of the IGBT modules is independent of the stresses experienced during its life cycle, that is, the order of the cyclic thermal stresses. Some of the nonlinear cumulative damage models presented in [52] could be more close to the reality due the self-accelerating effect along with the degradation of the IGBT modules. However, it still requires considerable validation efforts before applying them for the lifetime prediction of the IGBT modules. An improved way could consider the change of the electrothermal parameters due to degradation (e.g., the increase of the thermal impedance and on-state voltage of IGBT modules), which will result in an accelerated damage under the same loading condition and ambient condition. With the assumption of linear cumulative damage, Miner's rule is applied in this paper for the accumulated damage analysis of bond wires.

The whole life cycle can be divided into fractions for each datum of the mission profile data. Since the mission profile has been measured with a sampling rate of one second, the number of cycles per second due to line frequency power cycling is 50 ($f = 50$ Hz). Each consumption fraction is summed up to obtain the accumulated damage due to line frequency power cycling as follows:

$$\text{Damage}_{50} = \sum_i \frac{n_{i,50}}{N_{i,50}} \quad (6)$$

where $n_{i,50}$ is the number of temperature cycles due to the line frequency cycling and $N_{i,50}$ is the number of cycles to failure for the same cycle type and same stress as $n_{i,50}$.

The number of cycles to failure has been calculated based on (1) and (5) considering the load variations coming from the

TABLE II
ACCUMULATED DAMAGE PER YEAR DUE TO POWER CYCLING AND THERMAL CYCLING

Loading	t_{on}	Accumulated damage	Lifetime consumption
Line frequency	0.01 s	0.0257	2.57%
T_{amb} & SI	1 s–60 s	0.0027	0.27%

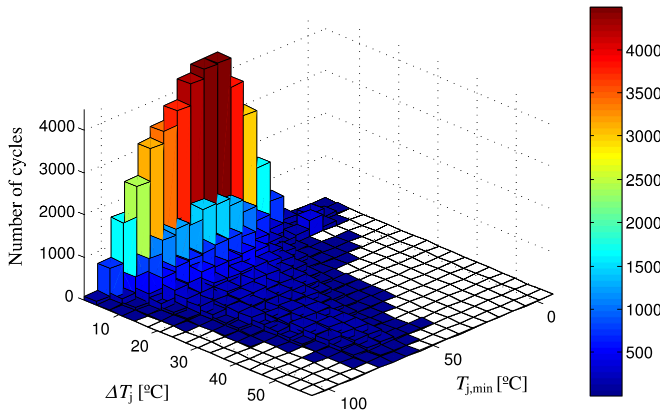

Fig. 11. Rainflow counting of the annual junction temperature profile: δT_j—junction temperature fluctuation, and $T_{j,\min}$—minimum junction temperature.

given mission profile. The junction temperature and its fluctuation are extracted from the mission profile for each measurement point. The heating time has a fixed periodicity ($t_{\mathrm{on}} = 0.01$ s) and the rest of the parameters (V, D, I) are kept constant. The obtained results are summarized in Table II. It is worth to note that the predicted lifetime consumption only considers the end-of-life of the bond wires. There are also other failure mechanisms of IGBT modules, such as base plate solder fatigue, chip solder fatigue, and single-event inducted catastrophic failure (e.g., short-circuit failure). The lifetime of an IGBT module depends on the summation of the accumulated failure of each kind of failure mechanism, of which bond wires contribute only part of it.

3) Accumulated Damage Analysis of Low-Frequency Thermal Cycling: The second type of cycling exposed by the IGBTs results from the solar irradiance and ambient temperature fluctuations. Since temperature cycles do not follow a repetitive pattern in terms of amplitude and duration, the cycle counting principle applied in the presented study is according to the Rainflow method described in [53]. Accordingly, the Rainflow codes are programmed by the authors, being one of the most popular cycle counting techniques used in fatigue analysis. Fig. 11 illustrates the distribution of junction temperature cycling obtained through the Rainflow counting algorithm.

Similarly, the linear cumulative damage model is applied to obtain the lifetime consumption due to low-frequency thermal cycling by means of (7). Notice that only temperature cycles with heating time durations below 60 s are taken into account

$$\mathrm{Damage}_{\mathrm{ST}} = \sum_i \frac{n_{i,\mathrm{ST}}}{N_{i,\mathrm{ST}}} \tag{7}$$

where $n_{i,\mathrm{ST}}$ is the number of cycles due to low-frequency thermal cycling and $N_{i,\mathrm{ST}}$ is the number of cycles to failure for the same cycle type and same stress as n_{ST}. The obtained results are summarized in Table II.

It is thus apparent that the accumulated damage corresponding to the low-frequency thermal cycling has less contribution to the bond wire end-of-life consumption than the line frequency power cycling, for the considered mission profile. One of the reasons is that the majority of the thermal cycles have very low amplitudes (ΔT_j) when the heating time is below 60 s.

D. Monte Carlo Based Analysis of the Variances in IGBT Parameters and Lifetime Model

This section investigates the reliability analysis of IGBTs by taking into account the long-term operation and the relevant parameter variations. Two types of uncertainties are considered: 1) parameter uncertainties in the applied lifetime model, and 2) parameter uncertainties due to manufacturing process variations among IGBTs with the same product part number. Regarding the first type of uncertainty, each lifetime model has its limitations due to the specific test conditions, device technologies, and failure mechanism considered. The applied lifetime model in this study, the Bayerer model presented in (1), is derived from the testing data presented in [23]. The variations of the constants in (1) and the boundaries of the testing conditions are available based on the data shown in [23]. Therefore, the uncertainty of the fitting coefficients corresponding to the junction temperature and its fluctuation (β_1 and β_2) are taken into account. The impact of current variation per bond wire may be caused by electromigration; nonetheless, this failure mechanism is unlikely in the field operation since it usually appears under the combination of high junction temperature and high current density [23], [24]. Regarding the second type of uncertainty, the end-of-life of a large population of IGBTs with the same specification and same product part number varies in field operations due to variances in the manufacturing process. The IGBT parameter variations are defined in the manufacturer datasheet with a typical maximum and minimum value (e.g., on-state voltage $V_{\mathrm{ce,on}}$). The variances in $V_{\mathrm{ce,on}}$ are taken into account in this analysis, since they have a direct effect on the IGBT conduction losses and therefore the T_j and ΔT_j.

The bond wire lifetime prediction is based on the empirical lifetime model of (1) combined with (5), the cumulative damage model of (6) and (7), and the long-term mission profile. Parameter variations have been analyzed individually and jointly. All the parameters in the analysis are modeled by means of normal probability distribution functions as shown in Fig. 12. β_1 and β_2 are assumed to have a 5% and 20% variation, respectively, with a 90% confidence level according to the accelerated testing data published in [23]. Consequently, the typical maximum and minimum value of $V_{\mathrm{ce,on}}$ is extracted from the datasheet provided by the IGBT module. The variation of $V_{\mathrm{ce,on}}$ leads to 5% variation of ΔT_j and a 0.66% variation of T_j for the power module in the analysis. Since the mission profile data are continuously changing over the whole year, the dynamical mission profile has been converted into an equivalent static one, which produces the same degradation [46].

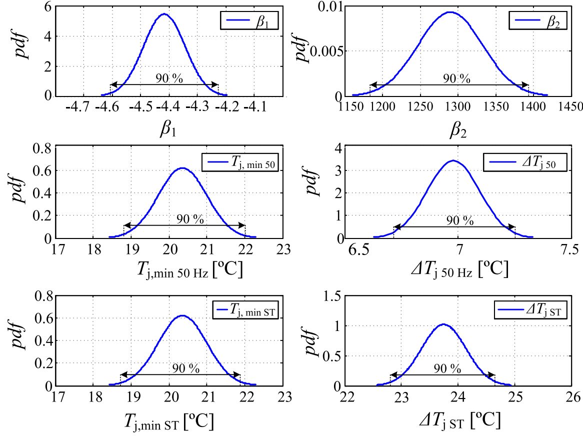

Fig. 12. Probability density functions of the parameters under analysis: β_1 and β_2 are the fitting coefficients of the applied lifetime model, $T_{j,\min 50}$ and $\Delta T_{j,50}$ are the minimum junction temperature and its fluctuation for the line frequency power cycling, and $T_{j,\min ST}$ and $\Delta T_{j,ST}$ are the minimum junction temperature and its fluctuation for the low-frequency thermal cycling.

TABLE III
EQUIVALENT STATIC VALUES FOR THE ANALYSIS OF THE VARIANCES IN IGBT PARAMETERS

	Line frequency	T_{amb} & SI
Average minimum junction temperature, ($T_{j,\min}$)	20.36 °C	20.36 °C
Accumulated damage per year, (Damage)	0.0257	0.0027
Number of cycles per year, (n)	1.57×10^9	72264
Heating time, (t_{on})	0.01 s	23.71 s
Number of cycles to failure, (N_f)	6.1×10^{10}	2.6×10^7
Junction temperature fluctuation, (ΔT_j)	6.98 °C	23.75 °C

The dynamical stresses are converted into static values for each type of temperature stress. The obtained results are summarized in Table III. The annual number of cycles to failure due to line frequency power cycling is calculated according to (6)

$$\text{Damage}_{50} = \sum_i \frac{n_{i,50}}{N_{i,50}}$$

$$N_{50} = \frac{1.57 \times 10^9}{0.0257} = 6.1 \times 10^{10} \text{ cycles per year.} \quad (8)$$

The equivalent junction temperature fluctuation due to line frequency power cycling during a year is

$$6.1 \times 10^{10} = 9.34 \times 10^{14} \times \Delta T_{j,50}^{-4.416} \times \exp\left(\frac{1290}{20.36 + 273}\right) \times 9.6 \times 10^{-4} \times \left(\frac{0.01}{1.5}\right)^{-0.3} \quad (9)$$

$$\Delta T_{j,50} = 6.98\,°\text{C}. \quad (10)$$

The annual number of cycles due to low-frequency thermal cycling are calculated from (7)

$$\text{Damage}_{ST} = \sum_i \frac{n_{i,ST}}{N_{i,ST}}$$

$$N_{ST} = \frac{72264}{0.0027} = 2.6 \times 10^7 \text{ cycles per year.} \quad (11)$$

The equivalent junction temperature fluctuation due to low-frequency thermal cycling during a year is

$$2.6 \times 10^7 = 9.34 \times 10^{14} \times \Delta T_{j,ST}^{-4.416} \times \exp\left(\frac{1290}{20.36 + 273}\right) \times 9.6 \times 10^{-4} \times \left(\frac{23.71}{1.5}\right)^{-0.3}. \quad (12)$$

$$\Delta T_{j,ST} = 23.75\,°\text{C}. \quad (13)$$

1) Individual Parameter Variation: A sensitivity analysis is carried out by considering individual parameter variations, while maintaining the other parameters to the mean of their distributions. The average minimum junction temperature $T_{j,\min}$, the junction temperature fluctuation ΔT_j, and the applied lifetime model parameters β_1 and β_2 have been modeled by normal probability distribution functions. The number of simulations is selected by considering the tradeoff between accuracy and the computation time. Therefore, 10.000 data points within the associated distributions are generated to build up the output accumulated damage distribution.

The lifetime consumption of the line frequency power cycling and the low-frequency thermal cycling is shown in Table III, each consumption fraction is summed up to obtain the total bond wire accumulated damage as

$$\text{Damage} = \text{Damage}_{50} + \text{Damage}_{ST} = 0.0284. \quad (14)$$

Fig. 13 shows the impact of individual parameters on the annual accumulated damage. The largest standard deviations are observed for the lifetime model parameters β_1 and β_2. It is now well highlighted the degree of importance to consider the uncertainties of the applied lifetime model parameters. Whereas β_1 and β_2 have a standard deviation of 0.0037 and 0.0083, respectively, T_j and ΔT_j have a standard deviation of 2.5×10^{-4} and 0.0019, respectively.

2) Variances in all Parameters: The second aspect of the study is to consider that all the parameters in the analyses could vary within the specified ranges as shown in Fig. 12. The accumulated damage distribution due to bond wire fatigue is given in Fig. 14 (a) with a population of 10.000 IGBTs. The accumulated failure due to bond wire of a single IGBT is between 0.017 to 0.048 out of 1 with a 90% confidence level. 10% of the IGBTs are predicted to have an annual damage less than 0.02 due to bond wire fatigue.

Fig. 14(b) and (c) illustrates the end-of-life distribution of bond wires due to fatigue. It can be noted that the estimated lifetime of a single IGBT is within 21 years to 60 years with a 90% confidence level. 1%, 5%, and 10% of the IGBTs are predicted to have failure due to bond wire fatigue after 17, 21, and 24 years, respectively as shown in Fig. 14(c).

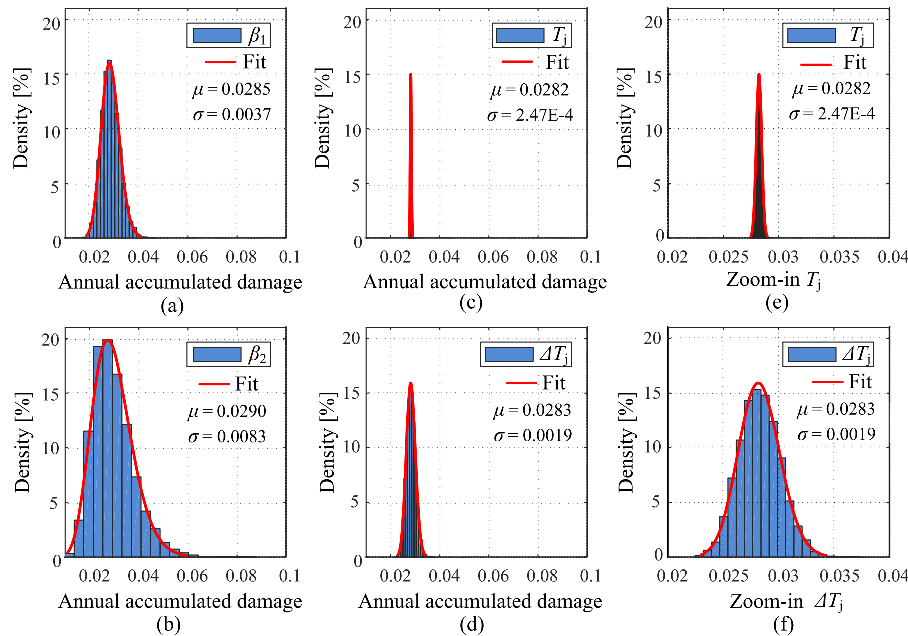

Fig. 13. Annual accumulated damage due to bond wire fatigue (μ—mean value; σ—standard deviation). (a) Lifetime model parameter β_1. (b) Lifetime model parameter β_2. (c) Minimum junction temperature T_j. (d) Junction temperature fluctuation ΔT_j. (e) Zoom-in minimum junction temperature T_j. (f) Zoom-in junction temperature fluctuation ΔT_j.

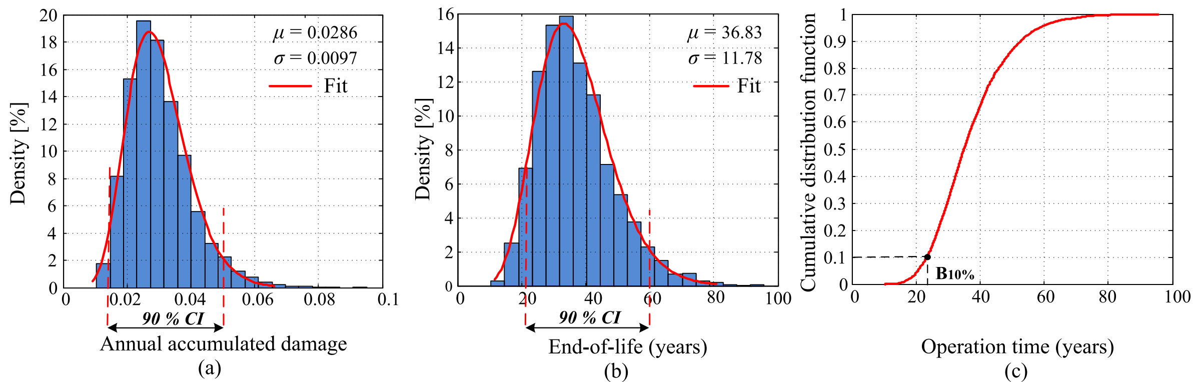

Fig. 14. Monte Carlo analysis based on bond wire fatigue (μ—mean value; σ—standard deviation). (a) Accumulated damage probability distribution function. (b) End-of-life probability distribution function. (c) End-of-life cumulative distribution function.

IV. Conclusion

The analysis in this paper has revealed a statistical approach for IGBT bond wire fatigue analysis and a guideline to evaluate its performance under relevant parameter variations. The impact of these variations has been evaluated by means of Monte Carlo simulations, and as a result, the accumulated failure due to bond wire fatigue and lifetime distribution with a specified confidence level are obtained. A case study on a 10-kW PV inverter has been presented with an experimentally verified power loss profile. The bond wires in the IGBTs have been estimated with a lifetime range from 21 to 60 years with a 90% confidence level. The predicted accumulated failure along with the long-term operation allows the PV inverter designers to have a risk analysis of unreliability. Moreover, the proposed method can be extended to different IGBT candidates to assist the selection of IGBTs. Therefore, PV inverter designers can select the most cost-effective IGBTs based on the cost information and the reliability specifications, avoiding either lack of robustness or overdesign with an unnecessary cost increase.

References

[1] H. Wang, M. Liserre, and F. Blaabjerg, "Toward reliable power electronics—Challenges, design tools and opportunities," *IEEE Ind. Electron. Mag.*, vol. 7, no. 2, pp. 17–26, Jun. 2013.

[2] B. Gu, J. Dominic, J.-S. Lai, C.-L. Chen, T. LaBella, and B. Chen, "High reliability and efficiency single-phase transformerless inverter for grid-connected photovoltaic systems," *IEEE Trans. Power Electron.*, vol. 28, no. 5, pp. 2235–2245, May 2013.

[3] E. Wolfgang, "Examples for failures in power electronics systems," in *Proc. ECPE Tut. Rel. Power Electron. Syst.*, Nuremberg, Germany, Apr. 2007, pp. 1842–1847.

[4] H. Wang, M. Liserre, F. Blaabjerg, P. de Place Rimmen, J. Jacobsen, T. Kvisgaard, and J. Landkildehus, "Transitioning to physics-of-failure as a reliability driver in power electronics," *IEEE J. Emerg. Sel. Topics Power Electron.*, vol. 2, no. 1, pp. 97–114, Mar. 2014.

[5] F. Chan and H. Calleja, "Reliability estimation of three single-phase topologies in grid-connected PV systems," *IEEE Trans. Ind. Electron.*, vol. 58, no. 7, pp. 2683–2689, Jul. 2011.

[6] S. De Leon-Aldaco, H. Calleja, F. Chan, and H. Jimenez-Grajales, "Effect of the mission profile on the reliability of a power converter aimed at photovoltaic applications - a case study," *IEEE Trans. Power Electron.*, vol. 28, no. 6, pp. 2998–3007, Jun. 2013.

[7] A. Ristow, M. Begovic, A. Pregelj, and A. Rohatgi, "Development of a methodology for improving photovoltaic inverter reliability," *IEEE Trans. Ind. Electron.*, vol. 55, no. 7, pp. 2581–2592, Jul. 2008.

[8] P. Zhang, Y. Wang, W. Xiao, and W. Li, "Reliability evaluation of grid-connected photovoltaic power systems," *IEEE Trans. Sustainable Energy*, vol. 3, no. 3, pp. 379–389, Jul. 2012.

[9] S. Dhople, A. Davoudi, A. Dominguez-Garcia, and P. Chapman, "A unified approach to reliability assessment of multiphase DC/DC converters in photovoltaic energy conversion systems," *IEEE Trans. Power Electron.*, vol. 27, no. 2, pp. 739–751, Feb. 2012.

[10] S. Harb and R. Balog, "Reliability of candidate photovoltaic module-integrated-inverter (PV-MII) topologies—A usage model approach," *IEEE Trans. Power Electron.*, vol. 28, no. 6, pp. 3019–3027, Jun. 2013.

[11] S. De Leon-Aldaco, H. Calleja, and J. Aguayo Alquicira, "Reliability and mission profiles of photovoltaic systems: A FIDES approach," *IEEE Trans. Power Electron.*, vol. 30, no. 5, pp. 2578–2586, May 2015.

[12] G. Petrone, G. Spagnuolo, R. Teodorescu, M. Veerachary, and M. Vitelli, "Reliability issues in photovoltaic power processing systems," *IEEE Trans. Ind. Electron.*, vol. 55, no. 7, pp. 2569–2580, Jul. 2008.

[13] *Military Handbook: Reliability Prediction of Electronic Equipment*, Standard MIL-HDBK-217F, Dec. 1991.

[14] J. Harms, *Revision of MIL-HDBK-217, Reliability Prediction of Electronic Equipment*, pp. 1–3, 2010.

[15] (2010, Sep.). *FIDES Guide 2009 Edition: A Reliability Methodology for Electronic Systems*. [Online]. Available: www.fides-reliability.org

[16] S. Yang, A. Bryant, P. Mawby, D. Xiang, L. Ran, and P. Tavner, "An industry-based survey of reliability in power electronic converters," in *Proc. Energy Convers. Cong. Expo.*, 2009, pp. 3151–3157.

[17] P. Ghimire, A. de Vega, S. Beczkowski, B. Rannestad, S. Munk-Nielsen, and P. Thogersen, "Improving power converter reliability: Online monitoring of high-power IGBT modules," *IEEE Ind. Electron. Mag.*, vol. 8, no. 3, pp. 40–50, Sep. 2014.

[18] V. Smet, F. Forest, J.-J. Huselstein, F. Richardeau, Z. Khatir, S. Lefebvre, and M. Berkani, "Ageing and failure modes of IGBT modules in high-temperature power cycling," *IEEE Trans. Ind. Electron.*, vol. 58, no. 10, pp. 4931–4941, Oct. 2011.

[19] J. Mecleish, *Enhancing MIL-HDBK-217 Reliability Predictions with Physics of Failure Methods*, pp. 1–6, Jan. 2010.

[20] A. Morozumi, K. Yamada, T. Miyasaka, S. Sumi, and Y. Seki, "Reliability of power cycling for IGBT power semiconductor modules," *IEEE Trans. Ind. Appl.*, vol. 39, no. 3, pp. 665–671, May 2003.

[21] A. Bryant, P. Mawby, P. Palmer, E. Santi, and J. Hudgins, "Exploration of power device reliability using compact device models and fast electrothermal simulation," *IEEE Trans. Ind. Appl.*, vol. 44, no. 3, pp. 894–903, May 2008.

[22] D. Hirschmann, D. Tissen, S. Schroder, and R. De Doncker, "Reliability prediction for inverters in hybrid electrical vehicles," *IEEE Trans. Power Electron.*, vol. 22, no. 6, pp. 2511–2517, Nov. 2007.

[23] R. Bayerer, T. Hermann, T. Licht, J. Lutz, and M. Feller, "Model for power cycling lifetime of IGBT modules—Various factors influencing lifetime," in *Proc. Int. Conf. Integr. Power Syst.*, 2008, pp. 1–6.

[24] L. Yang, P. Agyakwa, and C. Johnson, "Physics-of-failure lifetime prediction models for wire bond interconnects in power electronic modules," *IEEE Trans. Device Mater. Reliability*, vol. 13, no. 1, pp. 9–17, Mar. 2013.

[25] R. Schmidt and U. Scheuermann, "Separating failure modes in power cycling tests," in *Proc. Int. Conf. Integr. Power Electron. Syst.*, 2012, pp. 1–6.

[26] Y. Song and B. Wang, "Survey on reliability of power electronic systems," *IEEE Trans. Power Electron.*, vol. 28, no. 1, pp. 591–604, Jan. 2013.

[27] G. Walker, "Evaluating MPPT converter topologies using a Matlab PV model," *J. Electr. Electron. Eng. Australia*, vol. 21, no. 1, pp. 49–56, 2001.

[28] A. Volke and M. Hornkamp, *IGBT Modules*, 2nd ed., Infineon Technologies AG, Neubiberg, Germany, 2012.

[29] K. Ma, M. Liserre, F. Blaabjerg, and T. Kerekes, "Thermal loading and lifetime estimation for power device considering mission profiles in wind power converter," *IEEE Trans. Power Electron.*, vol. 30, no. 2, pp. 590–602, Feb. 2015.

[30] A. Wintrich, U. Nicolai, W. Tursky, and T. Reimann, *Application Manual Power Semiconductors*, Semikron International GmbH, Nuremberg, Germany, 2011.

[31] C. Sintamarean, F. Blaabjerg, H. Wang, and F. Iannuzzo, "Reliability oriented design tool for the new generation of grid connected PV inverters," *IEEE Trans. Power Electron.*, vol. 30, no. 5, pp. 2635–2644, May 2015.

[32] Y. Yang, H. Wang, F. Blaabjerg, and T. Kerekes, "A hybrid power control concept for PV inverters with reduced thermal loading," *IEEE Trans. Power Electron.*, vol. 29, no. 12, pp. 6271–6275, Dec. 2014.

[33] J. Wilde and E. Zukowski, "Probabilistic analysis of the influences of design parameter on the reliability of chip scale packages," pp. 1–8, Apr. 2006.

[34] C. Bailey, T. Tilford, and H. Lu, "Reliability analysis for power electronics modules," in *Proc. 30th Int. Spring Seminar Electron. Technol.*, 2007, pp. 12–17.

[35] C. Bailey, T. Tilford, S. Ridout, and H. Lu, "Optimizing the reliability of power electronics module isolation substrates," presented at the Int. Conf. Eng. Optim., Rio de Janeiro, Brazil, 2008.

[36] A. Alghassi, S. Perinpanayagam, M. Samie, and T. Sreenuch, "Computationally efficient, real-time, and embeddable prognostic techniques for power electronics," *IEEE Trans. Power Electron.*, vol. 30, no. 5, pp. 2623–2634, May 2015.

[37] Y. Yang, H. Wang, F. Blaabjerg, and K. Ma, "Mission profile based multi-disciplinary analysis of power modules in single-phase transformerless photovoltaic inverters," in *Proc. 15th Eur. Conf. Power Electron. Appl.*, Sep. 2013, pp. 1–10.

[38] Semikron. *SEMITOP 3 IGBT module—SK50GB12T4T*. [Online]. Available: http://www.semikron.com

[39] M. Iachello, V. De Luca, G. Petrone, N. Testa, L. Fortuna, G. Cammarata, S. Graziani, and M. Frasca, "Lumped parameter modeling for thermal characterization of high-power modules," *IEEE Trans. Compon., Packag. Manuf. Technol.*, vol. 4, no. 10, pp. 1613–1623, Oct 2014.

[40] T. Orlowska-Kowalska, F. Blaabjerg, and J. Rodriguez, *Advanced and Intelligent Control in Power Electronics and Drives*. Switzerland: Springer Int., 2014.

[41] M. Liserre, F. Blaabjerg, and S. Hansen, "Design and control of an *LCL*-filter-based three-phase active rectifier," *IEEE Trans. Ind. Appl.*, vol. 41, no. 5, pp. 1281–1291, Sep./Oct. 2005.

[42] T.-Y. Hung, L.-L. Liao, C. Wang, W. Chi, and K.-N. Chiang, "Life prediction of high-cycle fatigue in aluminum bonding wires under power cycling test," *IEEE Trans. Device Mater. Rel.*, vol. 14, no. 1, pp. 484–492, Mar. 2014.

[43] *IEC International Standard for Semiconductor Devices—Mechanical and Climatic test Methods—Power Cycling*, IEC 60747-34, 2005.

[44] *Technical Information IGBT Modules Use of Power Cycling Curves for IGBT 4*, Infineon, Neubiberg, Germany, 2012.

[45] M. Ikonen, "Power cycling lifetime estimation of IGBT power modules based on chip temperature modeling," Master's thesis, Lappeenranta Univ. Technol., Lappeenranta, Finland, 2012.

[46] J. McPherson, *Reliability Physics and Engineering*, 2nd ed. Switzerland: Springer Int., 2013.

[47] M. Held, P. Jacob, G. Nicoletti, P. Scacco, and M. H. Pech, "Fast power cycling test for IGBT modules in traction application," in *Proc. Power Electron. Drive Syst.*, vol. 86, no. 10, pp. 1193–1204, 1999.

[48] A. Syed, "Limitations of Norris-Landzberg equation and application of damage accumulation based methodology for estimating acceleration factors for Pb free solders," in *Proc. 11th Int. Conf. Thermal, Mech. Multi-Phys. Simulation, Exp. Microelectron. Microsyst.*, pp. 1–11, Apr. 2010.

[49] A. Fatemi and L. Yang, "Cumulative fatigue damage and life prediction theories: A survey of the state of the art for homogeneous materials," *Int. J. Fatigue*, vol. 20, no. 1, pp. 9–34, 1998.

[50] M. Miner, "Cumulative damage in fatigue," *J. Appl. Mech.*, vol. 12, pp. 159–164, 1945.

[51] M. F. Ashby and D. R. H. Jones, *Engineering Materials 1—An Introduction to Properties, Applications and Design*, 3rd ed. Oxford, U.K.: Butterworth-Heinemann, 2005, p. 228.

[52] H. Huang and P. Mawby, "A lifetime estimation technique for voltage source inverters," *IEEE Trans. Power Electron.*, vol. 28, no. 8, pp. 4113–4119, Aug. 2013.

[53] *Standard Practices for Cycle Counting in Fatigue Analysis*, ASTM Int. E1049-85, 2005.

Paula Diaz Reigosa (S'14) was born in Gijon, Spain. She received the B.S. degree in industrial engineering with a specialization in electrical engineering from the University of Oviedo, Oviedo, Spain, in 2012, and the M.S. degree in power electronics and drives from Aalborg University, Aalborg, Denmark, in 2014, where she is currently working toward the Ph.D. degree in failure mechanisms for power semiconductor devices. She was an intern master student in the Department of Wind Power Systems in Siemens, Aalborg, from June to September 2013 and with the Department of Reliability of Power Electronics in Danfoss, Graasten, Denmark, from September 2013 to January 2014.

Her current research interests include the reliability of power devices including power device failures, development of nondestructive testing facilities for assessment of high-power modules under extreme conditions, and emerging power electronics applications.

Huai Wang (S'07–M'12) received the B.E. degree from the Huazhong University of Science and Technology, Wuhan, China, in 2007, and the Ph.D. degree from the City University of Hong Kong, Hong Kong, in 2012.

He is currently an Associate Professor and a Work Package Leader with the Center of Reliable Power Electronics, Aalborg University, Aalborg, Denmark. He was a Visiting Scientist with the ETH Zurich, Zurich, Switzerland, from August to September, 2014 and with the Massachusetts Institute of Technology, Cambridge, MA, USA, from September to November, 2013. He was with the ABB Corporate Research Center, Baden, Switzerland, in 2009. His current research interests include the reliability of power electronic systems, reliability of capacitors and IGBT modules, multiobjective life-cycle performance optimization of power electronic systems, time-domain control of converters, and emerging power electronics applications. He has co-edited a book *Reliability of Power Electronic Converter Systems* (London, U.K.: IET, 2015), filed four patents, and contributed more than 30 journal papers.

Dr. Wang received six paper awards and project awards from industry, IEEE, and the Hong Kong Institution of Engineers. He also receives the Green Talents Award from the German Federal Ministry of Education and Research, in 2014. He serves the Guest Editor-in-Chief of the IEEE JOURNAL OF EMERGING AND SELECTED TOPICS IN POWER ELECTRONICS special issue on power electronics for energy efficient buildings and an Associate Editor of the IEEE TRANSACTIONS ON POWER ELECTRONICS.

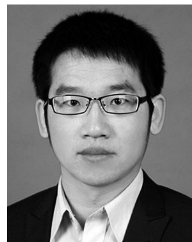

Yongheng Yang (S'12–M'15) received the B.Eng. degree from Northwestern Polytechnical University, Xi'an, China, in 2009, and the Ph.D. degree from Aalborg University, Aalborg, Denmark, in 2014. He was a Postgraduate with South-east University, Nanjing, China, from 2009 to 2011.

In 2013, he was a Visiting Scholar with the Department of Electrical and Computer Engineering, Texas A&M University, College Station, TX, USA. Since 2014, he has been with the Department of Energy Technology, Aalborg University, where he is currently an Assistant Professor. His research interests include grid integration and control of renewable energy systems, harmonics in adjustable speed drives and grid-connected power converters, and the reliability of power electronics.

Dr. Yang is involved in the IEEE Industry Applications Society student activities. He is a Committee Member of the IEEE Power Electronics Society Young Professionals and responsible for the webinar series. He serves as a Guest Associate Editor of the IEEE JOURNAL OF EMERGING AND SELECTED TOPICS IN POWER ELECTRONICS special issue on Power Electronics for Energy Efficient Buildings, and frequently as a Session Chair for various technical conferences.

Frede Blaabjerg (S'86–M'88–SM'97–F'03) received the Ph.D. degree from Aalborg University, Aalborg, Denmark, in 1992.

He was with ABB-Scandia, Randers, Denmark, from 1987 to 1988. He became an Assistant Professor in 1992, an Associate Professor in 1996, and a Full Professor of power electronics and drives in 1998 at Aalborg University. His current research interests include power electronics and its applications such as in wind turbines, photovoltaic systems, reliability, harmonics, and adjustable speed drives.

Dr. Blaabjerg has received 15 IEEE Prize Paper Awards, the IEEE Power Electronics Society Distinguished Service Award in 2009, the EPE-PEMC Council Award in 2010, the IEEE William E. Newell Power Electronics Award 2014, and the Villum Kann Rasmussen Research Award 2014. He was an Editor-in-Chief of the IEEE TRANSACTIONS ON POWER ELECTRONICS from 2006 to 2012. He has been Distinguished Lecturer for the IEEE Power Electronics Society from 2005 to 2007 and for the IEEE Industry Applications Society from 2010 to 2011.